Running title: NHX antiporters and auxin homeostasis

NHX antiporters regulate the pH of endoplasmic reticulum and auxin-mediated development

Ligang Fan[1], Lei Zhao[1], Wei Hu[1], Weina Li[1], Ondřej Novák[2], Miroslav Strnad[2], Sibu Simon[3], Jiří Friml[4], Jinbo Shen[5], Liwen Jiang[5] & Quan-Sheng Qiu[1]

[1]MOE Key Laboratory of Cell Activities and Stress Adaptations, School of Life Sciences, Lanzhou University, Lanzhou, Gansu, China, 730000;

[2]Laboratory of Growth Regulators, Centre of the Region Haná for Biotechnological and Agricultural Research, Institute of Experimental Botany AS CR & Palacký University, Šlechtitelů 27, CZ-78371 Olomouc, Czech Republic;

[3]Mendel Centre for Plant Genomics and Proteomics, Central European Institute of Technology (CEITEC), Masaryk University, Kamenice 5, CZ-625 00 Brno, Czech Republic;

[4]Institute of Science and Technology (IST) Austria, Am Campus 1, 3400 Klosterneuburg, Austria;

[5]School of Life Sciences, Centre for Cell & Developmental Biology and State Key Laboratory of Agrobiotechnology, The Chinese University of Hong Kong, Shatin, New Territories, Hong Kong, China

Corresponding author

Quan-Sheng Qiu, School of Life Sciences, Lanzhou University, Lanzhou, Gansu, China, 730000. Email: qiuqsh@lzu.edu.cn

This article has been accepted for publication and undergone full peer review but has not been through the copyediting, typesetting, pagination and proofreading process which may lead to differences between this version and the Version of Record. Please cite this article as doi: 10.1111/pce.13153

ABSTRACT

AtNHX5 and AtNHX6 are endosomal Na^+,K^+/H^+ antiporters that are critical for growth and development in *Arabidopsis*, but the mechanism behind their action remains unknown. Here, we report that AtNHX5 and AtNHX6, functioning as H^+ leak, control auxin homeostasis and auxin-mediated development. We found that *nhx5 nhx6* exhibited growth variations of auxin-related defects. We further showed that *nhx5 nhx6* was affected in auxin homeostasis. Genetic analysis showed that AtNHX5 and AtNHX6 were required for the function of the ER-localized auxin transporter PIN5. Although AtNHX5 and AtNHX6 were co-localized with PIN5 at ER, they did not interact directly. Instead, the conserved acidic residues in AtNHX5 and AtNHX6, which are essential for exchange activity, were required for PIN5 function. AtNHX5 and AtNHX6 regulated the pH in ER. Overall, AtNHX5 and AtNHX6 may regulate auxin transport across the ER via the pH gradient created by their transport activity. H^+-leak pathway provides a fine-tuning mechanism that controls cellular auxin fluxes.

Summary statement

This study aims to understand the mechanism underlying the function of the endosomal antiporters AtNHX5 and AtNHX6 in controlling plant development. We observed the auxin-related growth defects and auxin homeostasis alterations in *nhx5 nhx6* double mutants, which led to the discovery of the involvement of AtNHX5 and AtNHX6 in the function of the ER-localized auxin transporter PIN5. We demonstrated that AtNHX5 and AtNHX6 might regulate auxin transport across the ER via the pH gradient created by their transport activity. This study highlights the importance of AtNHX5 and AtNHX6, functioning as H^+ leak, in controlling auxin homeostasis and auxin-mediated development.

Key-words: *Arabidopsis*, endosomal Na^+,K^+/H^+ antiporters, AtNHX5, AtNHX6, auxin, PIN5, development, pH

INTRODUCTION

Plant Na^+,K^+/H^+ antiporters (NHX) transport protons (H^+) across a membrane in exchange for Na^+ or K^+. They are essential for cellular ion and pH homeostasis, and play significant roles in diverse cellular processes (Pardo *et al*. 2006; Bassil *et al*. 2012; Chanroj *et al*. 2012; Qiu 2012; Reguera *et al*. 2014). AtNHX5 and AtNHX6, which share high sequence similarity (78.7%), are endosomal NHX antiporters that are localized in the Golgi, TGN, and PVC (Yokoi *et al*. 2002; Pardo *et al*. 2006; Reguera *et al*. 2015; Qiu 2016a; Qiu 2016b). Studies showed that *nhx5 nhx6* double mutant was defective in development, having smaller rosettes and shorter seedlings (Bassil *et al*. 2011; Wang *et al*. 2015; Wu *et al*. 2016). How growth and development are regulated by AtNHX5 and AtNHX6, however, remains largely unknown.

The plant hormone auxin is a key regulator of development (Mockaitis & Estelle 2008; Vanneste & Friml 2009; Adamowski & Friml 2015; Salehin *et al*. 2015). A unique feature of auxin is in its deferential or asymmetry distribution in tissues, which is a trigger of development. The asymmetry distribution of auxin is generated by local auxin biosynthesis and directional intercellular auxin transport (Tanaka *et al*. 2006; Vanneste & Friml 2009; Friml 2010). The directional or polar auxin transport is mediated by the auxin transporters, including the auxin influx AUX1/LAX family, the auxin efflux PIN proteins, and the ABCB/PGP family (Adamowski & Friml 2015; Grones & Friml 2015).

In *Arabidopsis*, the PIN protein family consists of eight members that are divided into two groups: plasma membrane (PM)-localized PINs and endoplasmic reticulum (ER)-localized PINs (Wabnik *et al*. 2011; Viaene *et al*. 2013). The PM-PINs contain PIN1-PIN4, and PIN7, while the ER-PINs contain PIN5, PIN6 (also acting at the PM; Simon *et al*. 2016) and PIN8. ER-PINs mediate auxin transport between the ER lumen and the cytosol, and hence control auxin homeostasis of the cells (Friml & Jones 2010; Adamowski & Friml 2015; Grones & Friml 2015). PIN8 is significantly expressed in the male gametophyte,

and is crucial for pollen development (Dal Bosco *et al*. 2012; Ding *et al*. 2012). PIN6 is involved in nectar production, development of short stamens, and root growth and development acting at both the ER and PM (Bender *et al*. 2013; Cazzonelli *et al*. 2013; Simon *et al*. 2016). PIN5 functions in lateral root initiation, and in root and hypocotyl growth (Mravec *et al*. 2009). Moreover, PIN5 was shown to antagonize the action of PIN6 and PIN8 in intracellular auxin homoeostasis and leaf vein patterning (Ding *et al*. 2012; Sawchuk *et al*. 2013). However, the mechanism underlying the regulation of the ER-PIN function is unclear.

Cellular pH is a key regulator for the polar transport of auxin (Tanaka *et al*. 2006; Vanneste & Friml 2009; Adamowski & Friml 2015). According to the chemiosmotic model, auxin is protonated in the acidic apoplast. The protonated auxin, which is lipophilic, diffuses across the membrane. When entering into the cell, auxin is deprotonated in the neutral cytoplasm and retained inside the cell. The efflux of the deprotonated auxin is facilitated by the polarly localized efflux complexes (Adamowski & Friml 2015). Thus, the pH-induced auxin protonation/deprotonation is central to the polar transport of auxin. A genetic study has shown that the *Arabidopsis* H^+-PPase AVP1 regulates the apoplastic pH and consequently the polar auxin transport, indicating the importance of the H^+-PPase and the cellular pH maintained by this H^+-pump in the polar transport of auxin (Li *et al*. 2005; Tanaka *et al*. 2006). However, the mechanism governing auxin homeostasis remains to be studied.

Cellular or organelle pH homeostasis is maintained by the activity of both H^+-pumps and other anion or cation transporters (Demaurex 2002; Casey *et al*. 2010; Schumacher 2014). These anion or cation transporters, acting as either shunt conductance or proton-leaks, counter the cellular or organelle acidification generated by the H^+-pumps. They fine tune the action of the H^+-pumps and consequently the specific pH of the cytosol or the organelles (Casey *et al*. 2010; Schumacher 2014). In plants, the acidic pH of the organelles is maintained by the proton pumps V-ATPases and pyrophosphatase (Martinière *et al*. 2013;

Schumacher 2014). A recent study found that AtNHX5 and AtNHX6 may act as a H^+-leak system to counter the luminal acidification (Martinière *et al*. 2013), signifying their role in pH homeostasis. Since both AtNHX5 and AtNHX6 and ER-PINs are localized in the secretory pathway, it raises the question of whether AtNHX5 and AtNHX6 regulate the auxin transport activity of ER-PINs through adjusting pH homeostasis.

In this study, we investigated the role of AtNHX5 and AtNHX6 in regulating the function of the ER-localized auxin transporter PIN5. We found that *nhx5 nhx6* exhibited growth variations of auxin defects and alteration in auxin homeostasis. Genetic studies showed that AtNHX5 and AtNHX6 were required for PIN5 function. We found that AtNHX5 and AtNHX6 were co-localized with PIN5 at the ER. Two conserved acidic residues in AtNHX5 and AtNHX6 were identified to be essential for the regulation of PIN5 function. Moreover, *nhx5 nhx6* had a reduced pH in ER. We conclude that AtNHX5 and AtNHX6 regulate ER pH and thus have direct impact on PIN5-dependent auxin homeostasis and auxin-mediated development. H^+-leak pathway is important for the adjustment of cellular auxin fluxes in plants.

MATERIALS AND METHODS

Plant materials and growth conditions

Arabidopsis thaliana ecotypes Columbia (Col-0), T-DNA insertion lines *nhx5-1* (Wisc-DsLox345-348M8), *nhx6-1*(SALK_113129C) and their transgenic lines were used in this study. In the growth chamber, plants were grown on compost (Pindstrup Substrate, Latvia) and subirrigated with tap water. Greenhouse conditions were as follows: 16-h-light/8-h-dark cycles, light intensity 100 μmol s^{-1} m^{-2} photosynthetically active radiation, temperature 22℃, and relative humidity 50 ± 10%. For plate-grown plants, *Arabidopsis* seeds were sterilized with 20% (v/v) bleach and stratified at 4□ for 3 days in the dark. Seedlings

were grown vertically on 1/2 Murashige and Skoog (MS) medium containing 1% sucrose, 1% agar and respective drugs, pH 5.8.

GUS staining assay

DR5::GUS was obtained from Dr. Guilfoyle of University of Missouri, USA (Ulmasov *et al*. 1997). *DR5::GUS* was transformed into *nhx5*, *nhx6*, *nhx5 nhx6* backgrounds by genetic crossing. The seedlings grown on the 1/2 MS plates for 5 days were used for the histochemical GUS assay. The seedlings were immersed in GUS staining solution (50 mM Na-Phosphate buffer, pH 7.0, 1 mM EDTA, 0.1% Triton X-100, 2 mg/mL 5-bromo-4-chloro-3-indolyl-β-D-glucuronic acid (X-gluc), 5 mM ferricyanide, and 5 mM ferrocyanide), and incubated for 2h at 37°C. Then, the materials were washed with 75% ethanol to clear chlorophyll. The stained seedlings were photographed by the Olympus light microscope.

DR5::GFP assay

DR5::GFP was produced in the previous study (Benková *et al*. 2003). *DR5::GFP* was inserted into *nhx5*, *nhx6*, *nhx5 nhx6* backgrounds through genetic crossing. The seedlings were grown on the 1/2 MS plates for 5 days. The images were obtained with a Leica TCS SP5 laser scanning confocal microscope. Fluorescence signals for GFP (excitation 488nm, emission 500-535 nm) and FM4-64 (excitation 488nm, emission 610-660 nm) were detected in the embryo. Sequential scanning was used for double labelling to avoid crosstalk between channels.

Auxin flux assay

Auxin fluxes were measured using the Non-invasive Micro-test Technology (NMT-100,

YoungerUSA LLC, Amherst, MA) with ASET 2.0 (Science wares, Falmouth, MA) and iFluxes 1.0 Software (Younger USA, LLC). The IAA sensor construction and surface modification were based on the method of McLamore (McLamore *et al*. 2010). The IAA electrode was calibrated with 0, 20, 40, 60, 80 and 100 μM IAA in PBS buffer. Only electrodes with a linear calibration slope ($R^2 > 0.99$) were used. Fick's first law of diffusion ($J = -D \times \Delta C/\Delta X$) was used to calculate the auxin flux (*J*, free auxin flux; ΔC, concentration differences; ΔX, distance between two positions; *D*, diffusion coefficient, $D = 7 \times 10^{-6}$ cm^2 s^{-1}) (Mancuso *et al*. 2005; McLamore *et al*. 2010). 5-day-old seedlings were used for measurement. Microelectrodes were set near the root surface at different distances from the root apex, vibrating typically between 0 and 20 μm from the surface (ΔX = 20 μm). Four independent biological replicates were performed.

Quantification of IAA and IAA metabolites

Seeds were stratified at 4□ for 3 d in the darkness and then transferred to a phytotron set at 22□ with a 16-h-light/8-h-dark photoperiod in vertically oriented Petri dishes to grow for another 5 days. Five biological replicates of *Arabidopsis* seedlings, shoot and root tissues were grown separately for the wild type and each mutant line, harvested and immediately frozen in liquid nitrogen. Extraction and purification of auxin metabolites were carried out as described previously by Novák *et al*. (2012) with minor modifications. Briefly, frozen samples (5 mg fresh weight) were homogenized using a MixerMill (Retsch GmbH, Haan, Germany) and extracted in ice-cold 1 ml 50 mM sodium phosphate buffer (pH 7.0) containing 1% sodium diethyldithiocarbamate, deuterium and ^{13}C-labeled internal standards (5 pmol of $^{13}C_6$-IAA , $^{13}C_6$-oxIAA, $^{13}C_6$-IAAAsp and $^{13}C_6$-IAAGlu). The pH was adjusted to 2.7 with 1 M hydrochloric acid, and the samples were purified by solid phase extraction on hydrophilic-lipophilic balanced reversed-phase sorbent columns (Oasis® HLB, 1 cc/30 mg;

Waters, Milford, MA, USA) conditioned with 1 ml methanol, 1 ml water, and 0.5 ml sodium phosphate buffer (pH 2.7). After sample application, the column was washed with 2 ml 5% methanol and then eluted with 2 ml 80% methanol. All eluates were evaporated at 37°C to dryness *in vacuo* and dissolved in 30 µl of mobile phase prior to mass analysis using an Acquity UPLC® System and Xevo™ TQ MS (Waters) triple quadrupole mass spectrometer, operating in multiple reaction monitoring (MRM) mode. The linear range spanned at least five orders of magnitude with a correlation coefficient of 0.9989–0.9998. Five independent biological replicates of each mutant were used in the assay.

Construction of the pUBQ10-PIN5-GFP3 plasmid

To generate the *PIN5* overexpression lines, *PIN5-GFP3* was amplified from *35S::PIN5-GFP3* to produce the entry vector pDONR-PIN5-GFP3, using the primers in Table S1 (Mravec *et al*. 2009). Then, pDONR-PIN5-GFP3 was subcloned into the expression vector pUBQ10-GWR by the Gateway method (Invitrogen). The destination plasmid pUBQ10-PIN5-GFP3 was transformed into the GV3101 *A. tumefaciens* strain, and the resultant bacterial clone was used to transform the Col-0 by the floral dip procedure (Clough & Bent 1998). Transgenic plants were selected on the solid 1/2 Murashige and Skoog (MS) medium containing hygromycin (25 mg/L). Then, the homozygous T3 lines, confirmed by PCR and GFP fluorescence, were crossed with *nhx5*, *nhx6* or *nhx5 nhx6* mutants. The homozygous F3 lines were screened by PCR and by analyzing the resistance to hygromycin (25 mg/L). The PCR primers were used in Table S2.

Plants grown in the soil for 2 weeks were used to take the photos, and to perform the growth analysis. For fluorescence analysis, the seedlings were grown on the 1/2 MS plates for 5 days. The images were obtained with a Leica TCS SP5 laser scanning confocal microscope. Fluorescence signals for GFP (excitation 488nm, emission 500-535 nm) were detected in the

roots of seedlings.

Construction of the double overexpression lines of *PIN5* OE/*NHX5* OE or *PIN5* OE/*NHX6* OE

To express *AtNHX5* or *AtNHX6* genes into the *35S::PIN5-GFP3* lines (Mravec *et al*. 2009), *AtNHX5* or *AtNHX6* genes were cloned from the entry plasmids pDONR-NHX5 and pDONR-NHX6, produced in our previous study (Wang *et al*. 2015), and were then subcloned into the binary vector pBIB-RFP by the Gateway method (Invitrogen). The resultant constructs *35S::NHX5-RFP* and *35S::NHX6-RFP* were transformed into Col-0 by the floral-dip procedure mediated by the GV3101 agrobacterium (Clough & Bent 1998). Transgenic plants were selected on the solid 1/2 Murashige and Skoog (MS) medium containing hygromycin (25mg/L). Then, the homozygous T3 lines, which were confirmed by PCR and fluorescence analysis, were crossed with *35S::PIN5-GFP3* line. The homozygous F3 lines were obtained by analyzing the GFP fluorescence.

Plants grown in the soil for 2 weeks were used to take the photos, and to perform growth analysis. For fluorescence analysis, the seedlings were grown on the 1/2 MS plates for 5 days. The images were obtained with a Leica TCS SP5 laser scanning confocal microscope. Fluorescence signals for GFP (excitation 488 nm, emission 500-535 nm) and RFP (excitation 561 nm, emission 595-620 nm) were detected in the roots of seedlings. Sequential scanning was used to avoid crosstalk between channels.

To determine if the co-localization between AtNHX6 and PIN5 was random, the red channel of dual-color images was rotated 180° relative to the green image using Adobe Photoshop CS3 (Adobe Systems) (Konopka *et al*. 2008). The distance from each focus in the red channel to the nearest focus in the green channel was measured using ImageJ. All images for figures were processed in Adobe Photoshop CS3.

Generation of the point mutants of AtNHX5 and AtNHX6 and expression in *PIN5* OE lines

The point mutants were generated in our previous study (Wang *et al*. 2015). These point mutants of *AtNHX5* and *AtNHX6* genes were recombined into pUBC-RFP using Gateway technology (Invitrogen). RFP was fused at the C terminals of the mutated *AtNHX5* and *AtNHX6* genes. These plasmids were transformed into the GV3101 *A. tumefaciens* strain, and the resulting bacterial clones were used to transform *nhx5 nhx6* by the floral dip procedure. Transgenic plants were screened by 0.002% Basta after growing in soil for a week. The homozygous T3 lines, including pUBC-NHX5-RFP (*nhx5 nhx6*), pUBC-NHX5-D164N-RFP (*nhx5 nhx6*), pUBC-NHX5-D193N-RFP (*nhx5 nhx6*), pUBC-NHX6-RFP (*nhx5 nhx6*), pUBC-NHX6-D165N-RFP (*nhx5 nhx6*), and pUBC-NHX6-D194N-RFP (*nhx5 nhx6*), were crossed with pUBQ10-PIN5-GFP3 (*nhx5 nhx6*). Finally, the homozygous F3 lines, including pUBQ10-PIN5-GFP3/pUBC-NHX5-RFP (*nhx5 nhx6*), pUBQ10-PIN5-GFP3/pUBC-NHX5-D164N-RFP (*nhx5 nhx6*), pUBQ10-PIN5-GFP3/pUBC-NHX5-D193N-RFP (*nhx5 nhx6*), pUBQ10-PIN5-GFP3/pUBC-NHX6-RFP (*nhx5 nhx6*), pUBQ10-PIN5-GFP3/pUBC-NHX6-D165N-RFP (*nhx5 nhx6*), pUBQ10-PIN5-GFP3 /pUBC-NHX6-D194N-RFP (*nhx5 nhx6*), were validated by fluorescence and resistance screening (0.002% Basta and 25 mg/L hygromycin, respectively).

For phenotype analysis, the photos were taken and the diameter of the rosettes were calculated for the plants grown in soil for 2 weeks.

Subcellular localizations of AtNHX5 and AtNHX6 genes driven by the native promoters in *Arabidopsis*

To clone the native promoters of *NHX5* and *NHX6* genes, the genomic DNA was extracted from 7-day-old seedlings using the Plant Genomic DNA Extranction Kit (TaKaRa), and was used as templates for PCR amplification.

To clone the *NHX5* promoter, a 2088 bp upstream of the open reading frame was amplifie d by PCR with the primers (Table S3). The PCR products were cloned into the expression vector pBIB-GWR-GFP with the restriction sites HindIII and KpnI to obtain the vector pBIB-ProNHX5-GWR-GFP.

To clone the *NHX6* promoter, a 4293 bp upstream of the open reading frame was amplifi ed by PCR with the primers (Table S3). The PCR products were cloned into the expression vector pBIB-GWR-GFP with the restriction sites XbaI and KpnI to obtain the vector pBIB-ProNHX6-GWR-GFP.

NHX5 and *NHX6* genomic DNA sequences were amplified using the primers in Table S3. The PCR products were cloned into the entry vector pDONR/Zeo (Invitrogen) to produce the vectors pDONR-NHX5-GD and pDONR-NHX6-GD. Then, pDONR-NHX5-GD and pDONR-NHX6-GD were recombined into the expression vectors pBIB-ProNHX5-GWR-GFP and pBIB-ProNHX6-GWR-GFP using Gateway technology (Invitrogen) to obtain the vectors pBIB-ProNHX5-NHX5-GFP and pBIB-ProNHX6-NHX6-GFP, which were fused to the N-termini of GFP, driven by the native promoters. The resulting constructs were transformed into Agrobacterium tumefaciens GV3101, and were dipped into *nhx5 nhx6*. Transgenic plants were selected on the solid 1/2 Murashige and Skoog (MS) medium containing hygromycin (25 mg/L). The homozygous T3 lines were screened by analyzing the resistance to hygromycin.

To generate the double reporter lines, the ER marker *mCherry-HDEL* (from ABRC) were

introduced into the *NHX5::NHX5-GFP*/(*nhx5 nhx6*) or *NHX6::NHX6-GFP*/(*nhx5 nhx6*) lines by genetic cross. The GFP and mCherry signals were visualized in the roots of F1 seedlings by a Leica TCS SP5 laser scanning confocal microscope. The GFP excitation wavelength was 488 nm and emission was 500-535 nm; the mCherry excitation wavelength was 561 nm and emission was 600-630 nm. Sequential scanning was used for double labelling to avoid crosstalk between channels.

Co-immunoprecipitation assay

The transgenic plants co-expressing *35S::NHX5-RFP* with *35S::PIN5-GFP3* or co-expressing *35S::NHX6-RFP* with *35S::PIN5-GFP3* were used for co-immunoprecipitation assay. Total proteins were prepared from 4-week-old soil-grown plants. Leaves (2 g) were grinded in liquid nitrogen in 4 ml extraction buffer containing 50 mM HEPES-KOH, pH 7.5, 0.15 M NaCl, 0.5% (v/v) Triton X-100, 0.1% (v/v) Tween 20 and 1×plant protease inhibitor cocktail (Sangon, BS384). Homogenates were centrifuged at 10,000g for 15 min at 4°C to remove cellular debris. The supernatants were mixed with anti-RFP antibodies (MBL, M165-3) and incubated for 1 h at 4ºC with agitation. After incubation, 100 μl Protein-A/G PLUS-Agarose (Sangon, BS694) was added to precipitate the antigen-antibody complex. The beads were collected after overnight of incubation at 4ºC by centrifugation at 10,000g for 1 min. Then, the beads were washed for five times with 5 ml extraction buffer. At last, the antigen-antibody complex was eluted by boiling in 2× SDS loading buffer and run on a 10% SDS-PAGE gel. Proteins immunoprecipitated with anti-RFP antibodies were probed with anti-GFP antibodies (Roche, 11814460001).

pH measurement

For the measurement of ER pH, the protoplasts were prepared from 3-week-old Col-0 and

nhx5 nhx6 plants expressing the *PRpHluorin-HDEL* probe (Yoo *et al*. 2007; Shen *et al*. 2013). The PRpHluorin-HDEL signals at emission wavelength of 500 to 530 nm were recorded with dual-excitation wavelength at 405 and 488nm, respectively, and obtained a ratio 405nm/488nm to calculate the pH using the calibration curve. In vivo calibration was achieved from the same protoplasts expressing the *PRpHluorin* for pH measurement. To take the fluorescent image, protoplasts were incubated for 5 min in WI protoplast buffer (0.5 M mannitol and 20 mM KCl; Yoo *et al*. 2007) with 25 μM nigericin, 60 mM KCl, and 10 mM MES/HEPE Bis-Tris-propane, adjusted to various pH values ranging from 5.0 to 8.0 for each calibration point (Reguera *et al*. 2015; Martinière *et al*. 2013). Fluorescent images were acquired using the TCS SP5 laser scanning confocal microscope equipped with a 40×objective by the sequential line scanning mode. The pH profile of the protoplast was indicated by pseudocoloring images.

RESULTS

AtNHX5 and AtNHX6 regulate auxin-mediated growth in *Arabidopsis*

Firstly, we assessed the role of AtNHX5 and AtNHX6 in growth and development more deeply. Since AtNHX5 and AtNHX6 share high sequence similarity (78.7%) and are functional redundancy, neither *nhx5* nor *nhx6* single mutants showed any growth phenotype (Wang *et al*. 2015). We thus started our assay with the *nhx5 nhx6* double mutants generated in our previous study (Wang *et al*. 2015).

We found that *nhx5 nhx6* exhibited growth variations of hormonal defects. As shown in Fig.1a, in the early growth period, *nhx5 nhx6* had fewer branches (Fig. 1a). However, after growing for about 60 days, when the main branch stopped growing, *nhx5 nhx6* continued producing more side branches (Fig. 1a). As shown in Fig. 1b, from day 40 to day 60, the branch numbers of *nhx5 nhx6* increased 4.7 fold, while that of the wild type plants increased

only about 0.6 fold. This phenomenon manifested by the main branch inhibition of the side branch generation is a process typical of apical dominance, caused by the changes in auxin distribution in the seedlings (Skoog & Thimann 1934; Booker *et al*. 2003). Moreover, *nhx5 nhx6* was flowering early: the average flowering time for the wild type plants was 28 days while *nhx5 nhx6* was 25 days (Fig. 1c). The cotyledon of *nhx5 nhx6* was epinastic; the two cotyledons of *nhx5 nhx6* formed a narrower angle: the wild type plants formed an angle of 104°, while *nhx5 nhx6* was 84°, decreasing about 19% (Fig. 1d,e), similar to the PIN5 OX seedlings (Mravec *et al*. 2009). In addition, *nhx5 nhx6* produced longer hypocotyls: the hypocotyls of *nhx5 nhx6* were increased by18% compared to the wild type plants (Fig. 1d,f); hypocotyl growth is tightly controlled by auxin (Savaldi-Goldstein *et al*. 2008). Furthermore, *nhx5 nhx6* was sensitive to α-naphthaleneacetic acid (NAA) treatment. As shown in Fig. 1d,g, *nhx5 nhx6* generated more lateral roots under 100 nM NAA treatment: *nhx5 nhx6* produced 39% more lateral roots than the wild type plants, similar to the mutants involved in auxin homeostasis (Péret *et al*. 2009). Interestingly, the cotyledon angle and hypocotyl growth of *nhx5 nhx6* were not improved by NAA treatment (Fig. 1d). It has been known that exogenous application of auxin (either indole-3-acetic acid [IAA], 2,4-dichlorophenoxyacetic acid [2,4-D] or NAA) does not stimulate hypocotyl elongation, mainly due to the inefficient uptake and distribution of these compounds in cells (Savaldi-Goldstein *et al*. 2008).

To confirm the function of the *AtNHX5* and *AtNHX6* genes, we performed genetic complementation. RFP was fused with the C-terminus of the *AtNHX5* and *AtNHX6* genes and the constructs were introduced into the *nhx5 nhx6* double mutants (Wang *et al*. 2015). *ANHX5* or *AtNHX*6 restored the growth and development of the *nhx5 nhx6* seedlings to the wild-type level (Fig. 1a,d). These results suggest that the growth phenotypes of *nhx5 nhx6* described above are indeed caused by the defect in *ANHX5* and *AtNHX6* genes. However, overexpression of either *AtNHX5* or *AtNHX6* alone in wild-type plants did not enhance plant

growth (Fig. 1a,d), which is similar to our previous observation (Wang *et al*. 2015). The expression of the *AtNHX5* and *AtNHX6* genes in transgenic plants was confirmed by qRT-PCR (Supporting Information Fig. S1a,b).

Auxin distribution and homeostasis are altered in *nhx5 nhx6*

We next examined whether AtNHX5 and AtNHX6 were involved in auxin distribution and homeostasis. We first checked auxin levels in *nhx5 nhx6* using the auxin-responsive reporters DR5::GUS and DR5::GFP. The *DR5::GUS* or *DR5::GFP* cassette was transferred into *nhx5*, *nhx6*, and *nhx5 nhx6* through genetic crossing. The activity of DR5::GUS or DR5::GFP was examined either by histochemical staining or by observing GFP fluorescent signal. As shown in Fig. 2a, in the cotyledon, while DR5::GUS signal was unchanged in *nhx5* and *nhx6*, a significant change in DR5::GUS signal was observed in *nhx5 nhx6*. The highest DR5::GUS signal at the distal tip of the cotyledon became weaker in *nhx5 nhx6* compared to wild-type, while the DR5::GUS activity appeared in the central area of the cotyledon in *nhx5 nhx6*. Moreover, DR5::GFP signals were significantly brighter in the roots of both the single and double mutants relative to wild type, as shown in Fig. 2b,c. In particular, *nhx5* and *nhx6* single mutants generated strong signal in the stele of the roots, while *nhx5 nhx6* double mutants produced a significant signal in the lateral root cap. In addition, the DR5::GFP signals at the base of the embryo and at the tips of the developing cotyledons were distinctly weaker in *nhx5 nhx6* (Fig. 2d). Together, these results indicate that AtNHX5 and AtNHX6 are involved in auxin distribution and possibly auxin homeostasis in *Arabidopsis*.

We then determined the polar auxin transport in the root apex using the non-invasive microelectrode technique (NMT). NMT is a well-established tool for measuring root IAA influxes across the PM (Bailly *et al*. 2008; Henrichs *et al*. 2012). As shown in Fig. 3a, the auxin flux rate peaked at 200 μm from the root apex for both wild type and *nhx5 nhx6*.

Consistent with the high DR5::GFP activity in the roots of *nhx5 nhx6*, the mutant displayed a higher auxin influx activity at the root apex compared to the wild type (Fig. 3a).

To verify the role of AtNHX5 and AtNHX6 in regulating auxin homeostasis, we determined free auxin (IAA) levels in *nhx5*, *nhx6* and *nhx5 nhx6* using a liquid chromatography-tandem mass spectrometry (LC-MS/MS) analysis (Novák *et al*. 2012). As shown in Fig. 3b, while the free auxin was unchanged in the shoots of *nhx5 nhx6* mutants, a significant change in the free auxin was observed in the roots of *nhx5 nhx6*, suggesting the role of AtNHX5 and AtNHX6 in auxin homeostasis in roots. However, for *nhx5* and *nhx6* single mutants, no significant change in the free auxin level was observed in both shoots and roots, indicating functional redundancy between AtNHX5 and AtNHX6 (Fig. 3b).

We further analyzed IAA metabolism by LC-MRM-MS. Significant changes in IAA metabolism were observed in the roots of *nhx5 nhx6* compared to wild type: OxIAA was increased while IAA-Asp and IAA-Glu were decreased (Fig. 3c–e). Moreover, IAA-Asp in *nhx6* and IAA-Glu in *nhx5* were reduced in the shoots although IAA metabolism was unchanged in the shoots of most of the lines tested (Fig. 3c–e). IAA-Asp was increased in the roots of *nhx6* (Fig. 3d,e). These results suggest that AtNHX5 and AtNHX6 control auxin metabolism and homoeostasis.

AtNHX5 and AtNHX6 are required for PIN5 function in *Arabidopsis*

PIN5 is an ER-localized auxin transporter that regulates auxin homeostasis and seedling development in *Arabidopsis* (Mravec *et al*. 2009). Since AtNHX5 and AtNHX6 are endosomal NHX antiporters (Reguera *et al*. 2015; Wang *et al*. 2015), we reason that AtNHX5 and AtNHX6 may regulate PIN5 function and thus control auxin homeostasis and development.

A previous study has shown that overexpression of PIN5 suppresses growth and

produces dwarfed seedlings (Mravec *et al*. 2009). To check if AtNHX5 and AtNHX6 regulate PIN5 function, we examined the outcomes of overexpression of *PIN5* in *nhx5*, *nhx6* and *nhx5 nhx6* backgrounds. To this end, we first generated the 35S promoter driven-*PIN5* overexpression lines by introducing a *35S::PIN5-GFP3* plasmid into the mutant backgrounds. However, the fluorescence signal of PIN5-GFP was weak in *nhx5* or *nhx6* mutants and barely detected in *nhx5 nhx6* (Supporting Information Fig. S2a). qRT-PCR assay confirmed that *PIN5-GFP* expression was low in *nhx5* or *nhx6* mutants and not detectable in *nhx5 nhx6* (Supporting Information Fig. S2b), indicating silencing of *35S::PIN5-GFP3* in the mutant lines. We then generated a *PIN5* overexpression line by introducing a pUBQ10::PIN5-GFP3 plasmid into Col-0. We then overexpressed *PIN5* in the *nhx5*, *nhx6* and *nhx5 nhx6* backgrounds by crossing the pUBQ10::PIN5-GFP3/Col-0 line with the mutant plants. As shown in Fig. 4a,b, similar to Mravec *et al*. (2009), overexpression of *PIN5* in the Col-0 background suppressed the seedling growth. After growth in soil for two weeks, the diameter of the rosettes was reduced significantly for the Col-0 seedlings overexpressing *PIN5* (Fig. 4a,b). Overexpression of *PIN5* in the *nhx5* and *nhx6* single mutants also suppressed the seedling growth (Fig. 4a,b). However, the rosettes was unchanged for the *nhx5 nhx6* seedlings overexpressing *PIN5* (Fig. 4a,b). In addition, overexpression of *PIN5* promoted hypocotyl and lateral root growth in the wildtype and single mutants but the double mutants were unaffected (Fig. 4c-e). There was no defect in gravitropic response of root growth for either the mutants or the *PIN5* overexpression lines (Supporting Information Fig. S3a). Together, these results suggest that PIN5 function in controlling development requires the redundant action of AtNHX5 and AtNHX6.

Since overexpressing *PIN5* reduced the rosette size of the wildtype plants but did not affect the rosette of *nhx5 nhx6* (Fig.4 a,b), we reason overexpressing *AtNHX5* and *AtNHX6* may enhance PIN5 function to produce a tiny plant. To confirm this, we overexpressed

AtNHX5 and *AtNHX6* genes into *PIN5* overexpression lines (*PIN5* OE) to obtain the double overexpression lines *PIN5* OE/*NHX5* OE and *PIN5* OE/*NHX6* OE, respectively (Supporting Information Fig. S4a). The expression of *AtNHX5* and *AtNHX6* genes was driven by the 35S promoters in the double expression lines, and gene expression was confirmed by qRT-PCR (Supporting Information Fig. S1c). As shown in Supporting Information Fig. S4a,b, consistent with the above observations, overexpression of *PIN5* in the Col-0 background suppressed the seedling growth. Moreover, the double overexpression lines produced tiny plants that were even smaller than the *PIN5* OE line (Supporting Information Fig. S4a,b). It is noticeable that the *PIN5* OE line driven by the 35S promoter is much smaller than those driven by the UBQ10 promoter in Fig. 4a, which may due to a higher *PIN5* expression driven by the 35S promoter (Supporting Information Fig. S1d). In addition, the *PIN5* OE line was increased in hypocotyl and lateral root growth but hypocotyl and lateral root growth were significantly inhibited in the double expression lines (Supporting Information Fig. S4c,d). Again, the double expression lines did not have any defects in gravitropic response in root growth (Supporting Information Fig. S3b). In all, AtNHX5 and AtNHX6 are required for PIN5 function.

We then analyzed the expression and distribution of PIN5-GFP3 proteins in mutants and transgenic lines. As shown in Fig. 4f, a similar level of PIN5 proteins was observed in the wildtype and mutant seedlings as detected by western blot. The distribution of PIN5-GFP3 at the meristem region of the roots was observed under a confocal microscope. Bright GFP fluorescent signal in ER was observed for the wildtype and mutant seedlings overexpressing pUBQ10::PIN5-GFP3 (Fig. 4g). There is no significant difference between the mutant and wild type plants (Fig. 4g). In addition, the double expression lines had similar levels of PIN5 proteins and similar pattern of GFP fluorescent signals to the *PIN5* OE line (Supporting Information Fig. S4e,f). These results suggest that AtNHX5 and AtNHX6 may mediate PIN5

function without affecting the expression and distribution of PIN5.

AtNHX5 and AtNHX6 are co-localized with PIN5 at the ER

Since we found that AtNHX5 and AtNHX6 were required for the function of PIN5, which is localized at the ER, we were interested in examining whether AtNHX5 and AtNHX6 were co-localized with PIN5 at the ER. Studies have shown that AtNHX5 and AtNHX6 are localized at the Golgi, TGN and PVC (Bassil *et al*. 2011; Reguera *et al*. 2015; Wang *et al*. 2015). But these studies have not examined the localization of AtNHX5 and AtNHX6 in the ER.

To address this issue, we performed subcellular localization analysis with the stably transformed *Arabidopsis* seedlings that are co-expressed ER markers, in which *NHX5-GFP* and *NHX6-GFP* are driven by their native promoters. The double reporter lines were generated by crossing the transgenic lines *NHX5::NHX5-GFP*/*nhx5 nhx6* and *NHX6::NHX6-GFP*/*nhx5 nhx6* with the ER marker *mCherry-HDEL*. The co-localization of AtNHX5 and AtNHX6 with the ER marker *mCherry-HDEL* was observed at the meristem region of the roots, and was analyzed by the intensity correlation quotient (ICQ) and Pearson's correlation coefficient (PSC) approaches (Li *et al*. 2004; Reguera *et al*. 2015). As shown in Fig. 5a, AtNHX5-GFP was overlapped with the ER marker mCherry-HDEL (Table S5). AtNHX6-GFP was also co-localized with the ER marker mCherry-HDEL (Fig. 5a; Table S5), though the co-localization was low. These results suggest that AtNHX5 and AtNHX6 are localized to the ER.

We then examined if AtNHX5 and AtNHX6 are co-localized with PIN5 at the ER. We generated the double reporter lines by crossing the transgenic line *35S::PIN5-GFP3* with *35S::NHX5-RFP* or *35S::NHX6-RFP*. As shown in Fig. 5b, PIN5-GFP3 fluorescent signals were co-localized with AtNHX5-RFP or AtNHX6-RFP (Table S6), suggesting that AtNHX5

and AtNHX6 are co-localized with PIN5 at the ER. To eliminate the possibility that the co-localization between AtNHX6 and PIN5 was due to random overlap of the highly dense foci in the cells of meristematic region, the red channel image from thirteen different cells was rotated 180° with respect to the green channel, a technique for nonrandom co-localization analysis (Konopka *et al*. 2008). The average peak distance for the original images (4.89 pixels; n=150) was significantly different from that of the rotated images (10.68 pixels; n=150; $P < 0.0001$), indicating that the co-localization was statistically significant.

AtNHX5 and AtNHX6 do not interact physically with PIN5

We next examined whether AtNHX5 or AtNHX6 interacted physically with PIN5 by co-immunoprecipitation (Supporting Information Fig. S5). *NHX5-RFP* and *NHX6-RFP* were introduced into the *PIN5-GFP3* line by genetic cross. We first conducted immunoprecipitation with the anti-GFP monoclonal antibodies, followed by immunoblotting using anti-RFP antibodies. As shown in Fig. S5a, anti-GFP signal showed that PIN5-GFP was precipitated from *PIN5-GFP*, *NHX5-RFP/PIN5-GFP* and *NHX6-RFP/PIN5-GFP* lines. But no RFP signal was observed in either *NHX5-RFP/PIN5-GFP* or *NHX6-RFP/PIN5-GFP* lines. We then precipitated the samples with the anti-RFP monoclonal antibodies and immunoblotted with anti-GFP antibodies, as shown in Fig. S5b. Again, there was no GFP signal for either *NHX5-RFP/PIN5-GFP* or *NHX6-RFP/PIN5-GFP* lines. These results suggest that there is no physical interaction between PIN5 and AtNHX5 or AtNHX6.

The conserved acidic residues in AtNHX5 and AtNHX6 are essential for PIN5 function

Studies from bacteria, yeast and mammals have shown that the acidic amino acid residues in transmembrane domains of Na^+/H^+ antiporters are essential for ion transport activity (Fafournoux *et al.* 1994; Inoue *et al.* 1995; Dibrov *et al.* 1998). Our previous work has shown

that three of the conserved acidic residues of AtNHX5 (D164, E188, and D193) and AtNHX6 (D165, E189, and D194) are critical for their transport activity (Wang *et al*. 2015). Thus, we used the mutant genes of *AtNHX5* or *AtNHX6* to test whether the transport activity of AtNHX5 and AtNHX6 is required for PIN5 function.

We used the *nhx5 nhx6* double mutant with overexpressed *PIN5* as a testing system, as shown in Fig. 6, to examine if the transport activity of AtNHX5 and AtNHX6 is required for PIN5 function. The mutated *AtNHX5* or *AtNHX6* genes were transformed into *nhx5 nhx6* overexpressing *PIN5*, respectively, to check if they can rescue the phenotype. The mutations were made by replacing the acidic residues with the uncharged polar residues. In *AtNHX5*, D164 was mutated to N and D193 to N; in *AtNHX6*, D165 to N and D194 to N. Then, the wild type *AtNHX5* and *AtNHX6* genes as well as their mutated genes, including *NHX5-RFP, NHX5-D164N-RFP, NHX5-D193N-RFP, NHX6-RFP, NHX6-D165N-RFP,* and *NHX6-D194N-RFP*, were transformed into *nhx5 nhx6* bearing *PIN5*. Meanwhile, we used the transgenic lines transforming either the wild type or the mutated At*NHX5 and AtNHX6* genes without overexpressing *PIN5* as controls (Fig. 6a). The expression of *AtNHX5, AtNHX6* and their mutated genes in transgenic lines was confirmed by qRT-PCR (Supporting Information Fig. S1a,b). As shown in Fig. 6, overexpressing the wild type *AtNHX5* or *AtNHX6* gene in the *nhx5 nhx6/PIN5* OE produced a bigger plant compared to the *nhx5 nhx6*/*PIN5* OE, indicating that the transformed *AtNHX5* or *AtNHX6* gene functioned efficiently and thus mediated PIN5 function in development. However, seedling growth remained unchanged for those plants transformed with the mutated *AtNHX5* and *AtNHX6* genes (D164N and D193N of AtNHX5, and D165N and D194N of AtNHX6) (Fig. 6a,b), indicating that PIN5 is malfunctioning in these mutants. In addition, the double overexpression lines transforming the wild type *AtNHX5* or *AtNHX6* genes, *nhx5 nhx6/PIN5* OE/*NHX5* OE and the *nhx5 nhx6/PIN5* OE/*NHX6* OE, were smaller than their corresponding lines without overexpressing *PIN5*; but

the double overexpression lines transforming the mutated genes were unaltered compared to those without overexpressing *PIN5* (Fig. 6a,b). These results suggest that the transport activity of AtNHX5 and AtNHX6 is required for their regulation of the PIN5 function.

AtNHX5 and AtNHX6 regulate the pH in ER

Studies have shown that AtNHX5 and AtNHX6 regulate cellular pH (Bassil *et al*. 2011; Martinière *et al*. 2013; Wang *et al*. 2015). We are interested in examining if AtNHX5 and AtNHX6 regulate the pH in ER. We used the pHluorin-based pH sensor and the quantitative live-cell imaging technique to measure the luminal pH of the ER (Martinière *et al*. 2013; Shen *et al*. 2013). The ER-targeted pH sensor *PRpHluorin-HDEL* was transiently expressed in the *Arabidopsis* protoplasts. PRpHluorin contains an N-terminal signal peptide of aleurain from barley and the C-terminal amino acid sequence HDEL for retention in the ER (Shen *et al*. 2013). The protoplasts were prepared from the 3-week-old seedlings (Yoo *et al*. 2007; Shen *et al*. 2013). The calibration curve was created with the wild type protoplasts (Fig. 7a). As shown in Fig. 7b, the wild type plants had a pH of 7.37±0.22 in ER; there were no significant changes in either *nhx5* (pH 7.19±0.23) or *nhx6* (pH 7.24±0.28) compared to the wild type. However, *nhx5 nhx6* had a pH of 6.58±0.19 in ER, suggesting a more acidic pH in the ER of *nhx5 nhx6*. Interestingly, the pH was restored to the wild type level in either *nhx5 nhx6/NHX5* (7.43±0.22) or *nhx5 nhx6/NHX6* (7.34±0.24). Representative pseudocolored images of PRpHluorin-HDEL are shown in Fig. 7c. These results suggest that AtNHX5 and AtNHX6 regulate the pH in ER.

DISCUSSION

AtNHX5 and AtNHX6 regulate auxin homeostasis in *Arabidopsis*

Studies have shown that AtNHX5 and AtNHX6 are essential for growth and development in

Arabidopsis (Bassil *et al*. 2011; Wang *et al*. 2015). However, the molecular mechanism regarding the role of AtNHX5 and AtNHX6 in regulating plant development remains unclear. In this report, we found that *nhx5 nhx6* continued generating branches after the main branch stopped growing (Fig. 1a,b). Moreover, *nhx5 nhx6* flowered early; they had longer hypocotyls and epinastic cotyledons (Fig. 1c-f). Interestingly, *nhx5 nhx6* generated more lateral roots under NAA treatment (Fig. 1d,g). All these growth variations in *nhx5 nhx6* are typical of auxin defects. Furthermore, these growth defects in *nhx5 nhx6* were strongly supported by auxin homeostasis analysis. Our results indicated that *nhx5 nhx6* was affected in auxin homeostasis. We showed that DR5 activity was altered in the cotyledons (Fig. 2a), roots (Fig. 2b,c) and embryo (Fig. 2d) of *nhx5 nhx6*. Auxin influx activity (Fig. 3a) and free IAA (Fig. 3b) were high, and IAA metabolism (Fig. 3c-e) was altered in the roots of *nhx5 nhx6*. Together, these results suggest that AtNHX5 and AtNHX6 control auxin homeostasis and consequently the auxin-mediated growth and development in *Arabidopsis*.

Moreover, we noticed that the *nhx5* and *nhx6* single mutants were altered in IAA metabolism. For example, *nhx5* had reduced levels of IAA-Glu in the shoots (Fig. 3e); *nhx6* altered in IAA-Asp levels in both the shoots and shoots (Fig. 3d). However, the *nhx5* and *nhx6* single mutants did not show any defects in auxin-related growth phenotypes. Although the real reason behind this observation remains to be studied, we found that the levels of free IAA, the active form of auxin, were unaltered in the *nhx5* and *nhx6* single mutants (Fig. 3b). In addition, both the DR5::GUS and DR5::GFP signals showed that either there was no or only a slight change in auxin levels in the *nhx5* and *nhx6* single mutants (Fig. 2). These results indicate that knockout either the *NHX5* or *NHX6* gene alone would not cause a dramatic change in auxin metabolism and homeostasis that could lead to a visible phenotype alteration, which is due to functional redundancy between AtNHX5 and AtNHX6.

The transport activity of AtNHX5 and AtNHX6 is required for PIN5 function

Studies have shown that AtNHX5 and AtNHX6 are localized at the Golgi, TGN and PVC (Bassil *et al*. 2011; Reguera *et al*. 2015; Wang *et al*. 2015). In addition, it is reported that PIN5, PIN6 and PIN8 are ER-localized PIN proteins and facilitate auxin transport between the ER lumen and the cytosol (Friml & Jones 2010; Adamowski & Friml 2015; Grones & Friml 2015). In this study, our genetic analysis showed that PIN5 function in controlling development depended on AtNHX5 and AtNHX6. In the absence of AtNHX5 and AtNHX6, PIN5 lost its activity in inhibiting seedling growth (Fig. 4), while overexpressing *AtNHX5* and *AtNHX6* enhanced PIN5 function (Supporting Information Fig. S4a,b). How is PIN5 regulated by AtNHX5 and AtNHX6? Is it possible that AtNHX5 and AtNHX6 are localized at ER and regulate the activity of the ER-PINs? Confocal analysis showed that NHX5-GFP and NHX6-GFP were co-localized with the ER marker mCherry-HDEL (Fig. 5a), indicating the localization of AtNHX5 and AtNHX6 in the ER. More importantly, we found that AtNHX5 and AtNHX6 were co-localized with PIN5 at ER (Fig. 5b).

Then, how do AtNHX5 and AtNHX6 regulate PIN5 function? Via transport activity or physical interaction. Co-immunoprecipitation assay showed that there was no physical interaction between PIN5 and AtNHX5 or AtNHX6 (Supporting Information Fig. S5). We further found that PIN5 lost its activity in suppressing seedling growth when the conserved acidic residues were mutated for both *AtNHX5* and *AtNHX6* genes (Fig. 6), indicating that it is their transport activity that is required for the PIN5 function.

Since AtNHX5 and AtNHX6 are H^+-coupled cotransporters, their biochemical activity is transferring Na^+ or K^+ across a membrane in exchange for protons (H^+). Therefore, AtNHX5 and AtNHX6 function in maintaining pH and ion homeostasis in *Arabidopsis* (Bassil *et al*. 2011; Reguera *et al*. 2015; Wang *et al*. 2015). The above- mentioned results that AtNHX5 and AtNHX6 regulate PIN5 function by their transport activity, thus, may suggest that the

PIN5 function is regulated by the pH and/or ion homeostasis facilitated by AtNHX5 and AtNHX6. We indeed found that *nhx5 nhx6* had a reduced pH in ER (Fig. 7), indicating that AtNHX5 and AtNHX6 regulate ER pH. These results strongly support the notion that AtNHX5 and AtNHX6 may regulate PIN5 function via pH created by their transport activity. Nevertheless, the pH dependency of PIN5 transport activity needs to be demonstrated directly in future by the biochemical assays using the isolated membrane vesicles.

Growth analysis indicated that the *NHX5* OE or *NHX6* OE lines displayed a suppression but not an enhancement phenotype in hypocotyl and lateral root growth (Supporting Information Fig. S4c,d). While the detailed mechanism awaits further investigation, one thing is clear: overexpression of *AtNHX5* or *AtNHX6* is not necessary to enhance PIN5 activity and thus plant development. That is because PIN5 may need an appropriate pH to function properly, similar to the optimum pH for enzyme activities. Lacking or having more AtNHX5 or AtNHX6 would allow either less or more H^+ movement across the ER, leading to a pH alteration in ER. This altered ER pH, which is not appropriate for PIN5, would disturb PIN5 activity and thus its function in development. Therefore, investigating the mechanism regarding the interaction between AtNHX5 or AtNHX6 and PIN5 is an interesting topic that worth further study.

H^+-leak pathway is critical for auxin homeostasis in *Arabidopsis*

It is becoming evident that cellular or organelle pH homeostasis is maintained by both the activity of H^+-pumps and H^+-leak pathways (Demaurex 2002; Casey *et al*. 2010; Schumacher 2014). While the role of H^+-pumps in maintaining pH homeostasis has been widely studied, the function of the H^+-leak pathways is just starting to be explored (Schumacher 2014; Kondapalli *et al*. 2015). In animals, Na^+/H^+ antiporters have been reported to conduct H^+ leak to counter organelle acidification in order to maintain an optimal pH (Demaurex 2002;

Orlowski & Grinstein 2007). Kondapalli *et al*. (2013) reported that the human Na^+/H^+ exchanger NHE9 functions as a H^+-leak pathway in endosomes, and acts as a brake against excessive luminal acidification. They further found that NHE9, which functions as a H^+-leak pathway, limits luminal acidification to circumvent EGFR turnover and prolong downstream signaling pathways that drive tumor growth and migration (Kondapalli *et al*. 2015). In plants, similar to their animal counterparts, AtNHX5 and AtNHX6 may act as a H^+-leak system to counter the luminal acidification (Martinière *et al*. 2013). These results suggest that the Na^+/H^+ antiporters that function as H^+-leak system play an important role in growth and development in both animals and plants.

It is well known that auxin homeostasis is regulated by cellular pH. While *Arabidopsis* H^+-PPase AVP1, the vacuolar H^+ pump, which functions in maintaining cellular pH required for auxin homeostasis, has been identified (Li *et al*. 2005), the H^+-leak pathway that fine tunes the cellular pH for auxin homeostasis has not been identified. In this study, we demonstrated for the first time that AtNHX5 and AtNHX6, functioning as a H^+ leak, regulate auxin homeostasis and hence auxin-mediated development. Our results demonstrate that H^+-leak pathway plays an important role in auxin homeostasis in plants, adding an additional layer of fine-tuning of intercellular and intracellular auxin fluxes.

ACCESSION NUMBERS

Sequence data from this article can be found in the *Arabidopsis* Genome Initiative or GenBank/EMBL databases under the following accession numbers: *NHX5* (AT1G54370), *NHX6* (AT1G79610), *PIN5* (AT5G16530).

ACKNOWLEDGEMENTS

This work was supported by the National Basic Research Program of China (973 project, 2013CB429904 to QSQ), the National Natural Science Foundation of China (NSFC)

(31571464, 31371438, 31070222 to QSQ), the Research Fund for the Doctoral Program of Higher Education of China (RFDP) (20130211110001 to QSQ), and the Ministry of Education, Youth and Sports of the Czech Republic (the National Program for Sustainability I No. LO1204). We thank Dr. Tom J. Guilfoyle for DR5::GUS line, and Dr. Jia Li for pBIB-RFP vector and DR5::GFP line. We thank Liping Guan and Yang Zhao for their help with the confocal microscope assay.

REFERENCES

Adamowski M. & Friml J. (2015) PIN-dependent auxin transport: action, regulation, and evolution. *Plant Cell* **27**, 20-32.

Bailly A., Sovero V., Vincenzetti V., Santelia D., Bartnik D., Koenig B.W., ..., Geisler M. (2008) Modulation of P-glycoproteins by auxin transport inhibitors is mediated by interaction with immunophilins. *The Journal of Biological Chemistry* **283**, 21817-21826.

Bassil E., Coku A. & Blumwald E. (2012) Cellular ion homeostasis: emerging roles of intracellular NHX Na^+/H^+ antiporters in plant growth and development. *Journal of Experimental Botany* **63**, 5727-5740.

Bassil E., Ohto M.A., Esumi T., Tajima H., Zhu Z., Cagnac O., ..., Blumwald E. (2011) The *Arabidopsis* intracellular Na^+/H^+ antiporters NHX5 and NHX6 are endosome associated and necessary for plant growth and development. *Plant Cell* **23**, 224-239.

Bender R.L., Fekete M.L., Klinkenberg P.M., Hampton M., Bauer B., Malecha M., ..., Carter C.J. (2013) PIN6 is required for nectary auxin response and short stamen development. *Plant Journal* **74**, 893-904.

Benková E., Michniewicz M., Sauer M., Teichmann T., Seifertová D., Jürgens G. & Friml, J. (2003) Local, efflux-dependent auxin gradients as a common module for plant organ formation. *Cell* **115**, 591-602.

Booker J., Chatfield S. & Leyser O. (2003). Auxin acts in xylem-associated or medullary cells to mediate apical dominance. *Plant Cell* **15**, 495-507.

Casey J.R., Grinstein S., & Orlowski J. (2010). Sensors and regulators of intracellular pH. *Nature Reviews Molecular Cell Biology* **11,** 50-61.

Cazzonelli C.I., Vanstraelen M., Simon S., Yin K., Carron-Arthur A., Nisar N., ..., Pogson B.J. (2013) Role of the *Arabidopsis* PIN6 auxin transporter in auxin homeostasis and auxin-mediated development. *PLoS One* **8,** e70069.

Chanroj S., Wang G., Venema K., Zhang M.W., Delwiche C.F. & Sze H. (2012) Conserved and diversified gene families of monovalent cation/H^+ antiporters from algae to flowering plants. *Frontiers in Plant Science* **3,** 25.

Clough S.J. & Bent A.F. (1998) Floral dip: a simplified method for Agrobacterium-mediated transformation of *Arabidopsis thaliana*. *Plant Journal* **16,** 735-43.

Dal Bosco C., Dovzhenko A., Liu X., Woerner N., Rensch T., Eismann M., ..., Palme K. (2012) The endoplasmic reticulum localized PIN8 is a pollen-specific auxin carrier involved in intracellular auxin homeostasis. *Plant Journal* **71,** 860-870.

Demaurex N. (2002) pH Homeostasis of cellular organelles. *News in Physiological Sciences* **17,** 1-5.

Dibrov P., Young P.G. & Fliegel L. (1998) Functional analysis of amino acid residues essential for activity in the Na^+/H^+ exchanger of fission yeast. *Biochemistry* **37,** 8282-8288.

Ding Z., Wang B., Moreno I., Dupláková N., Simon S., Carraro N., ..., Friml J. (2012) ER-localized auxin transporter PIN8 regulates auxin homeostasis and male gametophyte development in *Arabidopsis*. *Nature Communications* **3,** 941.

Fafournoux P., Noël J. & Pouysségur J. (1994) Evidence that Na^+/H^+ exchanger isoforms NHE1 and NHE3 exist as stable dimers in membranes with a high degree of specificity for homodimers. *Journal of Biological Chemistry* **269,** 2589-2596.

Friml J. (2010) Subcellular trafficking of PIN auxin efflux carriers in auxin transport. *European Journal of Cell Biology* **89,** 231-235.

Friml J. & Jones A.R. (2010) Endoplasmic reticulum: the rising compartment in auxin biology. *Plant Physiology* **154,** 458-462.

Grones P. & Friml J. (2015) Auxin transporters and binding proteins at a glance. *Journal of Cell Science* **128,** 1-7.

Henrichs S., Wang B., Fukao Y., Zhu J., Charrier L., Bailly A., ..., Geisler M. (2012) Regulation of ABCB1/PGP1-catalysed auxin transport by linker phosphorylation. *EMBO Journal* **31,** 2965-2980.

Inoue H., Noumi T., Tsuchiya T. & Kanazawa H. (1995) Essential aspartic acid residues, Asp-133, Asp-163 and Asp-164, in the transmembrane helices of a Na^+/H^+ antiporter (NhaA) from Escherichia coli. *FEBS Letters* **363**, 264-268.

Kondapalli K.C., Llongueras J.P., Capilla-González V., Prasad H., Hack A., Smith C., ..., Rao R. (2015) A leak pathway for luminal protons in endosomes drives oncogenic signalling in glioblastoma. *Nature Communications* **6,** 6289.

Kondapalli K.C., Hack A., Schushan M., Landau M., Ben-Tal N. & Rao R. (2013) Functional evaluation of autism-associated mutations in NHE9. *Nature Communications* **4,** 2510.

Konopka C.A., Backues S.K. & Bednarek S.Y. (2008) Dynamics of Arabidopsis dynamin-related protein 1C and a clathrin light chain at the plasma membrane. *Plant Cell* **20**, 1363-1380.

Li Q., Lau A., Morris T.J., Guo L., Fordyce C.B. & Stanley E.F. (2004) A syntaxin 1, $G\alpha_o$, and N-type calcium channel complex at a presynaptic nerve terminal: analysis by quantitative immunocolocalization. *Journal of Neuroscience* **24,** 4070-4081.

Li J., Yang H., Peer W.A., Richter G., Blakeslee J., Bandyopadhyay A., ..., Gaxiola R. (2005) *Arabidopsis* H^+-PPase AVP1 regulates auxin-mediated organ development. *Science* **310,**

121-125.

Mancuso S., Marras A.M., Magnus V. & Baluska F. (2005) Noninvasive and continuous recordings of auxin fluxes in intact root apex with a carbon nanotube-modified and self-referencing microelectrode. *Analytical Biochemistry* **34,** 344-351.

Martinière A., Bassil E., Jublanc E., Alcon C., Reguera M., Sentenac H., ..., Paris N. (2013) In vivo intracellular pH measurements in tobacco and *Arabidopsis* reveal an unexpected pH gradient in the endomembrane system. *Plant Cell* **25,** 4028-4043.

McLamore E.S., Diggs A., Calvo Marzal P., Shi J., Blakeslee J.J., Peer W.A., ..., Porterfield D.M. (2010) Non-invasive quantification of endogenous root auxin transport using an integrated flux microsensor technique. *Plant Journal* **63**, 1004-1016.

Mockaitis K. & Estelle M. (2008) Auxin receptors and plant development: a new signaling paradigm. *Annual Review of Cell and Developmental Biology* **24,** 55-80.

Mravec J., Skůpa P., Bailly A., Hoyerová K., Krecek P., Bielach A., ..., Friml J. (2009) Subcellular homeostasis of phytohormone auxin is mediated by the ER-localized PIN5 transporter. *Nature* **459,** 1136-1140.

Novák O., Hényková E., Sairanen I., Kowalczyk M., Pospíšil T. & Ljung K. (2012) Tissue-specific profiling of the *Arabidopsis thaliana* auxin metabolome. *Plant Journal* **72,** 523-536.

Orlowski J. & Grinstein S. (2007) Emerging roles of alkali cation/proton exchangers in organellar homeostasis. *Current Opinion in Plant Biology* **19,** 483-492.

Pardo J.M., Cubero B., Leidi E.O. & Quintero F.J. (2006) Alkali cation exchangers: roles in cellular homeostasis and stress tolerance. *Journal of Experimental Botany* **57,** 1181-1199.

Péret B., De Rybel B., Casimiro I., Benková E., Swarup R., Laplaze L., ..., Bennett M.J. (2009) *Arabidopsis* lateral root development: an emerging story. *Trends in Plant Science* **14,** 399-408.

Qiu Q.S. (2012) Plant and yeast NHX antiporters: roles in membrane trafficking. *Journal of Integrative Plant Biology* **54,** 66-72.

Qiu Q.S. (2016a) Plant endosomal NHX antiporters: Activity and function. *Plant signaling & behavior* **11,** e1147643.

Qiu Q.S. (2016b) AtNHX5 and AtNHX6: Roles in protein transport. *Plant signaling & behavior* **11,** e1184810.

Reguera M., Bassil E. & Blumwald E. (2014) Intracellular NHX-type cation/H^+ antiporters in plants. *Molecular Plant* **7,** 261-263.

Reguera M., Bassil E., Tajima H., Wimmer M., Chanoca A., Otegui M.S., ..., Blumwald E. (2015) pH Regulation by NHX-Type Antiporters Is Required for Receptor-Mediated Protein Trafficking to the Vacuole in *Arabidopsis*. *Plant Cell* **27,** 1200-1217.

Salehin M., Bagchi R. & Estelle M. (2015) SCFTIR1/AFB-based auxin perception: mechanism and role in plant growth and development. *Plant Cell* **27,** 9-19.

Savaldi-Goldstein S., Baiga T.J., Pojer F., Dabi T., Butterfield C., Parry G., ..., Chory J. (2008) New auxin analogs with growth-promoting effects in intact plants reveal a chemical strategy to improve hormone delivery. *Proceedings of the National Academy of Sciences* **105,** 15190-15195.

Sawchuk M.G., Edgar A. & Scarpella E. (2013) Patterning of leaf vein networks by convergent auxin transport pathways. *PLoS Genetics* **9,** e1003294.

Schumacher K. (2014) pH in the plant endomembrane system-an import and export business. *Current Opinion in Plant Biology* **22,** 71-76.

Shen J., Zeng Y., Zhuang X., Sun L., Yao X., Pimpl P. & Jiang L. (2013) Organelle pH in the *Arabidopsis* endomembrane system. *Molecular Plant* **6,** 1419-1437.

Simon S., Skůpa P., Viaene T., Zwiewka M., Tejos R., Klíma P., ..., Friml J. (2016) PIN6 auxin transporter at endoplasmic reticulum and plasma membrane mediates auxin

homeostasis and organogenesis in *Arabidopsis*. *New Phytologist* **211**, 65-74.

Skoog F. & Thimann K.V. (1934) Further Experiments on the Inhibition of the Development of Lateral Buds by Growth Hormone. *Proceedings of the National Academy of Sciences* **20,** 480-485.

Tanaka H., Dhonukshe P., Brewer P.B. & Friml J. (2006) Spatiotemporal asymmetric auxin distribution: a means to coordinate plant development. *Cellular and molecular life sciences* **63,** 2738-2754.

Ulmasov T., Murfett J., Hagen G. & Guilfoyle T.J. (1997) Aux/IAA proteins repress expression of reporter genes containing natural and highly active synthetic auxin response elements. *Plant Cell* **9,** 1963-1971.

Vanneste S. & Friml J. (2009) Auxin: a trigger for change in plant development. *Cell* **136,** 1005-1016.

Viaene T., Delwiche C.F., Rensing S.A. & Friml J. (2013) Origin and evolution of PIN auxin transporters in the green lineage. *Trends in Plant Science* **18,** 5-10.

Wabnik K., Kleine-Vehn J., Govaerts W. & Friml J. (2011) Prototype cell-to-cell auxin transport mechanism by intracellular auxin compartmentalization. *Trends in Plant Science* **16,** 468-475.

Wang L., Wu X., Liu Y. & Qiu Q.S. (2015) AtNHX5 and AtNHX6 Control Cellular K^+ and pH Homeostasis in *Arabidopsis*: Three Conserved Acidic Residues Are Essential for K^+ Transport. *PLoS One* **10,** e0144716.

Wu X., Ebine K., Ueda T. & Qiu Q.S. (2016) AtNHX5 and AtNHX6 are required for the subcellular localization of the SNARE complex that mediates the trafficking of seed storage proteins in *Arabidopsis*. *PLoS One* **11,** e0151658.

Yokoi S., Quintero F.J., Cubero B., Ruiz M.T., Bressan R.A., Hasegawa P.M. & Pardo J.M. (2002) Differential expression and function of *Arabidopsis thaliana* NHX Na^+/H^+

antiporters in the salt stress response. *Plant Journal* **30,** 529-539.

Yoo S.D., Cho Y.H. & Sheen J. (2007) *Arabidopsis* mesophyll protoplasts: a versatile cell system for transient gene expression analysis. *Nature Protocols* **2,** 1565-1572.

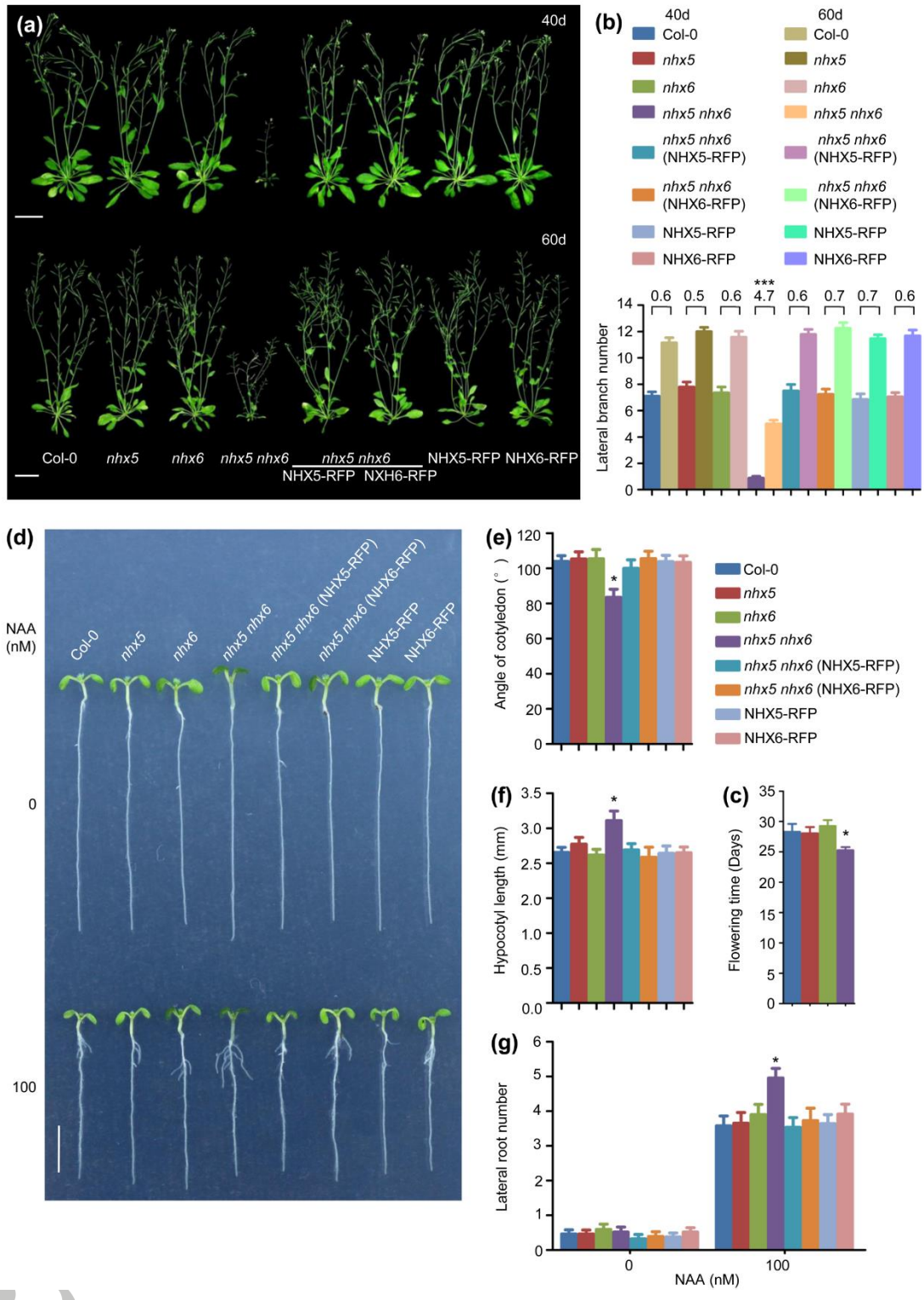

Figure 1. *nhx5 nhx6* exhibits growth variations of auxin defects.

(a) Plant growth. Pictures were taken for plants grown in the soil for 40 or 60 days.

(b) Branch numbers. The branches were counted from the 40- and 60-day-old plants as shown in a (mean ± SEM; $n \geqslant 30$). Scale bar, 4 cm.

(c) Flowering time. The flowering time is defined the time the seedling starts flowering in the text (mean ± SEM; $n \geqslant 30$).

(d-g) Seedling growth. (d) Phenotypes of seedlings. Pictures were taken for the 7-day-old seedlings. Scale bar, 0.5 cm. (e) Angles of cotyledons. The angles between the two cotyledons were measured for the 7-day-old seedlings (mean ± SEM; $n \geqslant 30$). (f) Hypocotyl length. Hypocotyl length was measured for the 7-day-old seedlings (mean ± SEM; $n \geqslant 30$). (g) Lateral roots. The number of lateral roots was measured for the seedlings treated with 100 nM NAA for 7 days (mean ± SEM; $n \geqslant 30$). (b,c and e-f) Statistics by *t* test are shown; $*P < 0.05$, $***P < 0.001$.

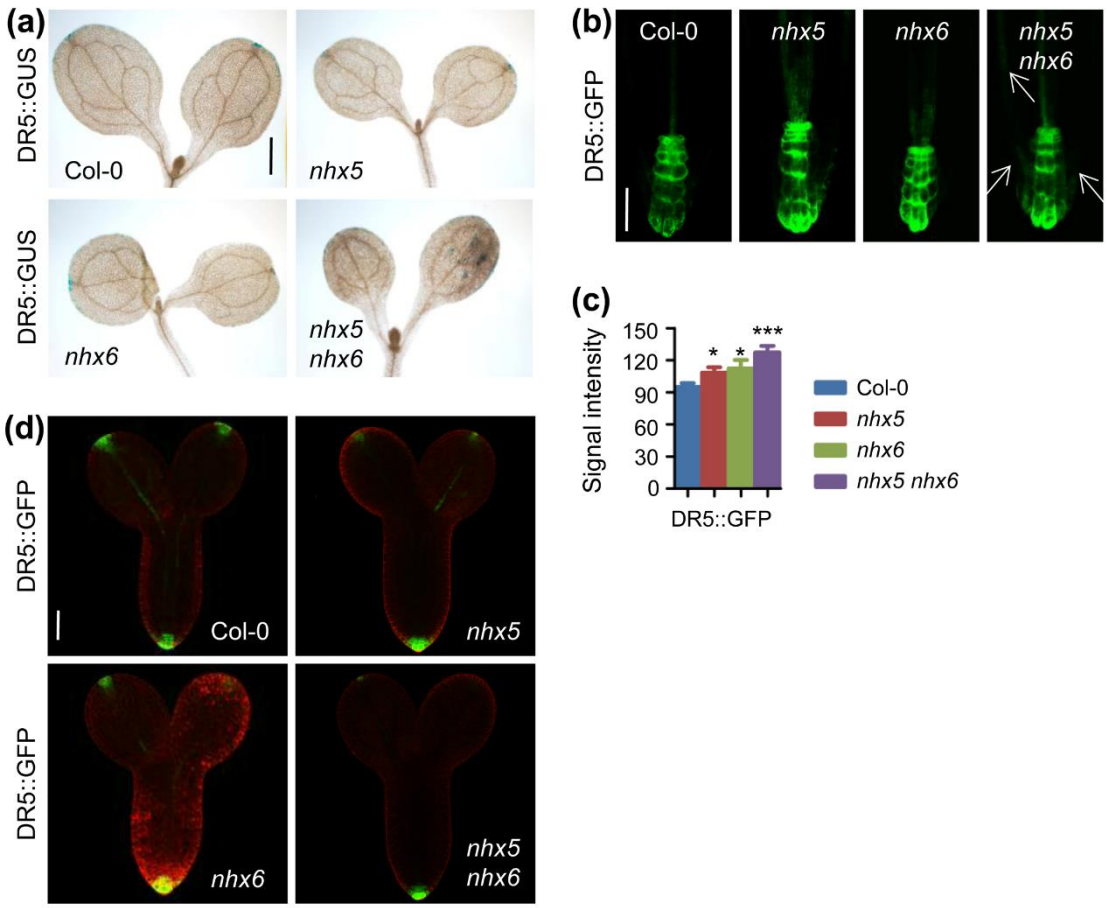

Figure 2. Auxin distribution and expression are altered in *nhx5 nhx6*.

(a) DR5::GUS staining. 5-day-old seedlings were stained with 2 mg/ml X-Gluc for 2h before microscope analysis. Scale bar, 0.5 mm.

(b) Confocal images of DR5::GFP in roots. 5-day-old seedlings were used in the assay. Scale bar, 40 μm.

(c) Signal intensity of DR5::GFP in roots (mean ± SEM; $n \geqslant 20$). Statistics by *t* test are shown; $*P < 0.05$, $***P < 0.001$.

(d) Confocal images of DR5::GFP in embryos. Images were taken at the late heart stage. Embryos were stained with 20 μg/ml FM4-64 for 5 min. Scale bar, 40 μm.

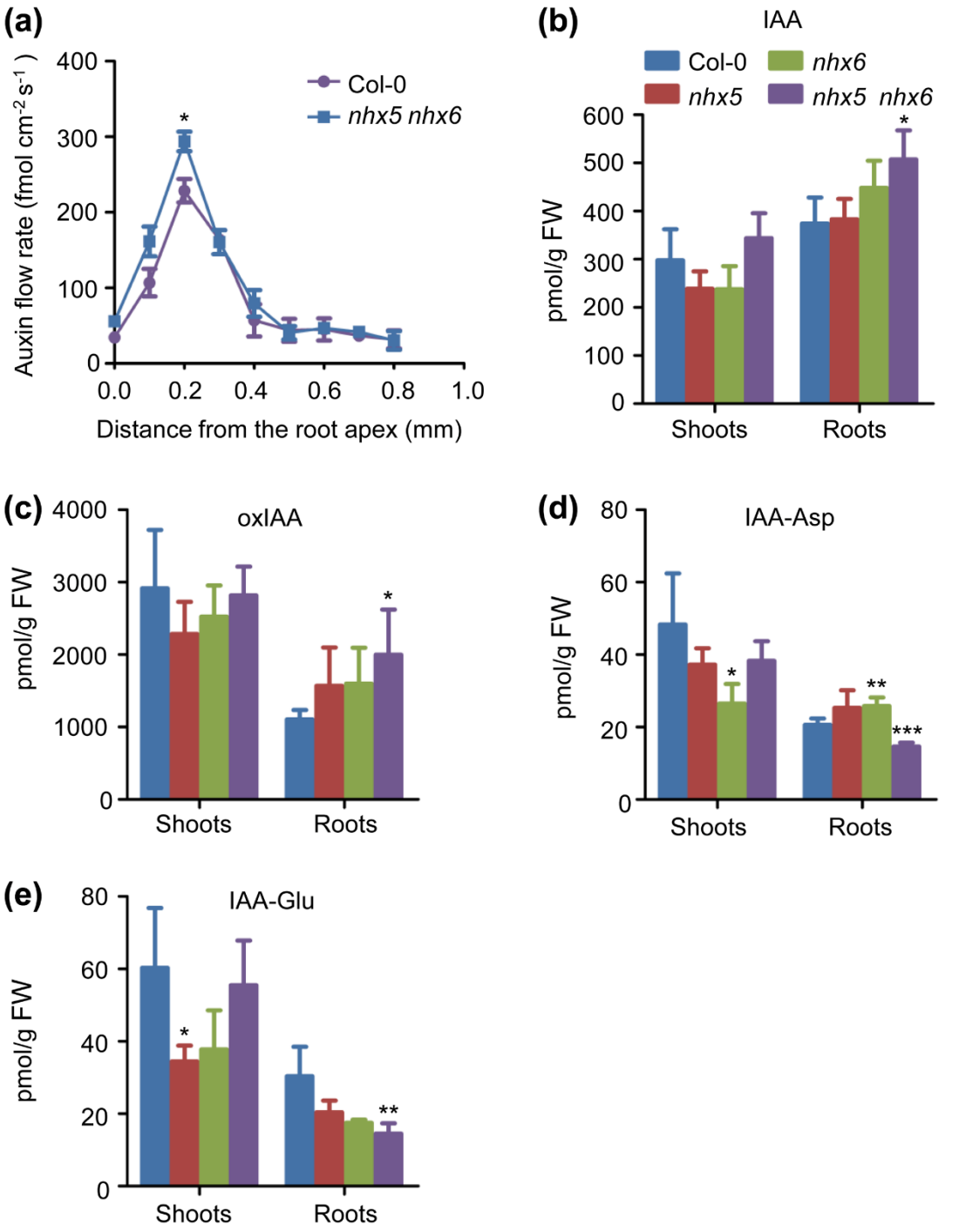

Figure 3. Auxin transport and IAA metabolism are defective in *nhx5 nhx6*.

(a) Auxin flux activity. Auxin flux was measured by NMT for 5-day-old seedlings; Four independent biological replicates were performed (mean ± SEM; $n = 4$). Statistics by *t* test are shown; $*P < 0.05$.

(b-e) Free IAA and IAA metabolite analysis by LC-MS/MS. The shoots and roots of 5-day-old seedlings were used in the assay (mean ± SEM; $n = 4$). (b) Free IAA. (c) Oxindole-3-acetic acid (OxIAA). (d) Indole-3-acetyl-aspartate (IAA-Asp). (e) Indole-3-acetyl-glutamate (IAA-Glu). (a-e) Statistics by *t* test are shown; $*P < 0.05$, $**P < 0.01$, $***P < 0.001$.

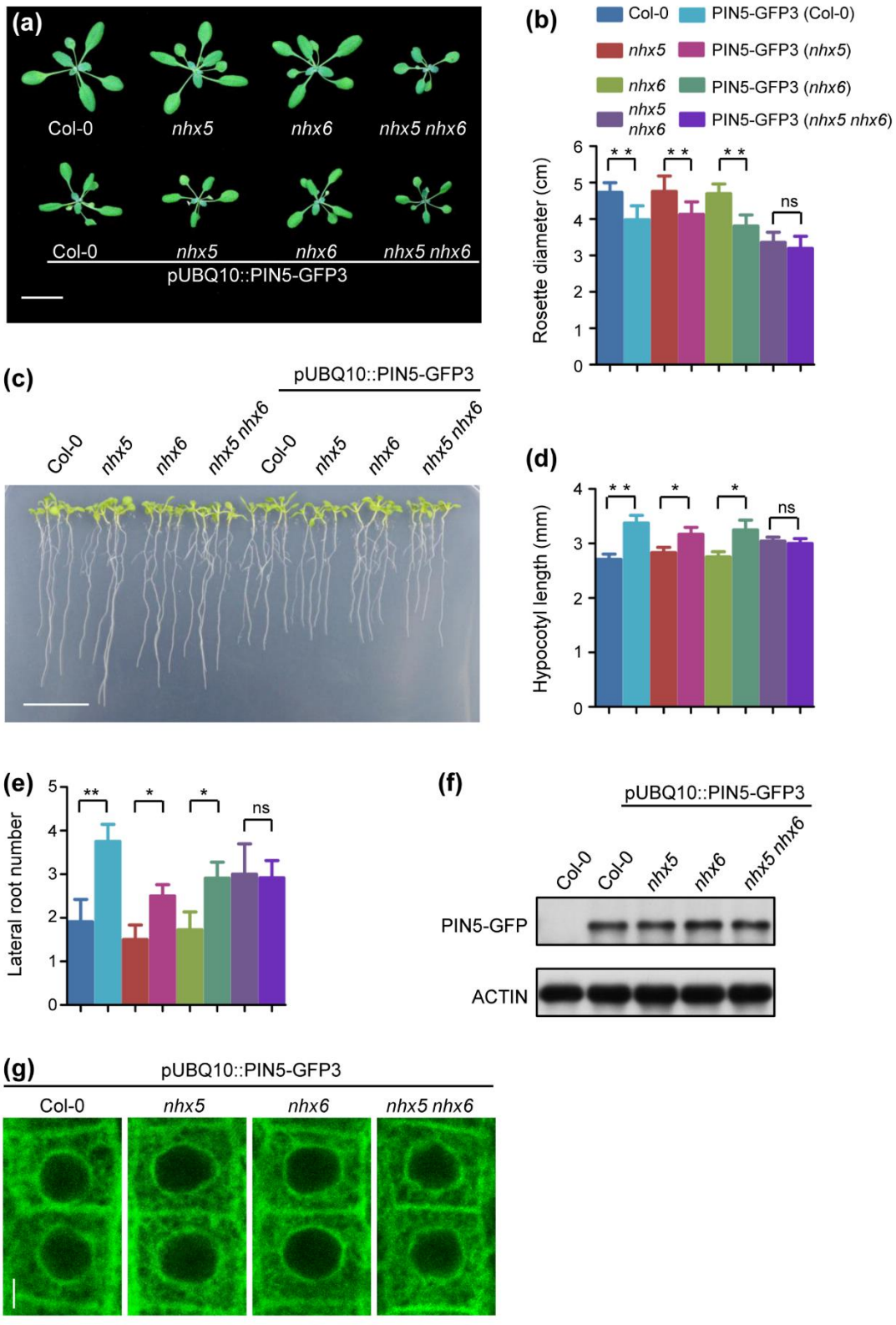

Figure 4. PIN5 function depends on AtNHX5 and AtNHX6.

(a,b) PIN5 was not functioning without AtNHX5 and AtNHX6. pUBQ10::PIN5-GFP3 was overexpressed in the *nhx5*, *nhx6* and *nhx5 nhx6* backgrounds. Pictures were taken from plants

grown for 2 weeks. (a) Growth phenotype of transgenic seedlings. Scale bar, 2 cm. (b) Diameter of the rosettes (mean ± SEM; $n \geqslant 30$). Statistics by *t* test are shown; $^{**}P < 0.01$. (c-e) Seedling growth. Plant growth was analyzed for the 7-day-old seedlings. (c) Phenotypes of seedlings. Scale bar, 1 cm. (d) Hypocotyl length. (mean ± SEM; $n \geqslant 20$). (e) Lateral roots. (mean ± SEM; $n \geqslant 20$). Statistics by *t* test are shown; $^{*}P < 0.05$, $^{**}P < 0.01$. (f) PIN5-GFP levels. Total proteins were extracted from 7-day-old seedlings. PIN5-GFP was detected by anti-GFP, and anti-ACTIN was a reference control.

(g) PIN5-GFP distribution. The GFP fluorescent signals were detected from the meristematic region of roots by confocal microscope for the 5-day-old seedlings. Scale bar, 10 μm.

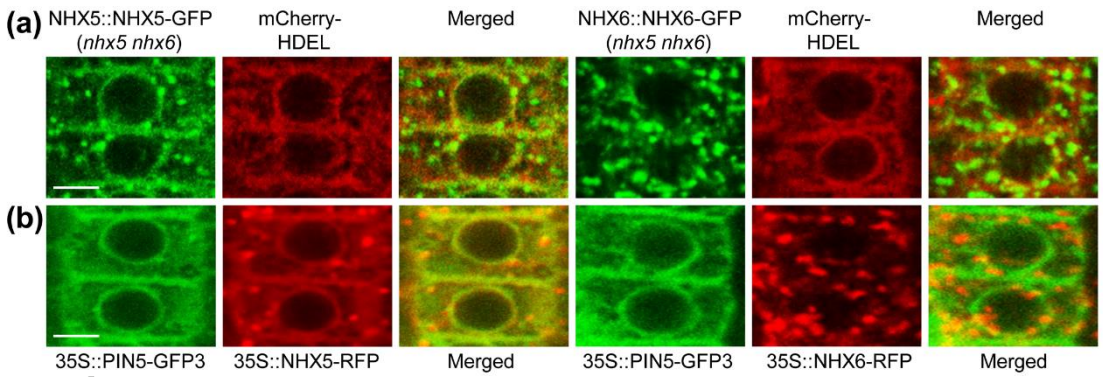

Figure 5. AtNHX5 and AtNHX6 are co-localized with PIN5 at the ER.

(a) Co-localization of AtNHX5 or AtNHX6 with ER marker. NHX5-GFP or NHX6-GFP (green) was co-expressed with the ER marker mCherry-HDEL (red). The fluorescent signal was detected by confocal microscope for the F1 seedlings grown for 5 days. Scale bar, 10 μm.

(b) Co-localization of AtNHX5 or AtNHX6 with PIN5. NHX5-RFP (red) or NHX6-RFP (red) was co-expressed with PIN5-GFP3 (green). The fluorescent signal was detected by confocal microscope for the F1 seedlings grown for 5 days. Scale bar, 10 μm.

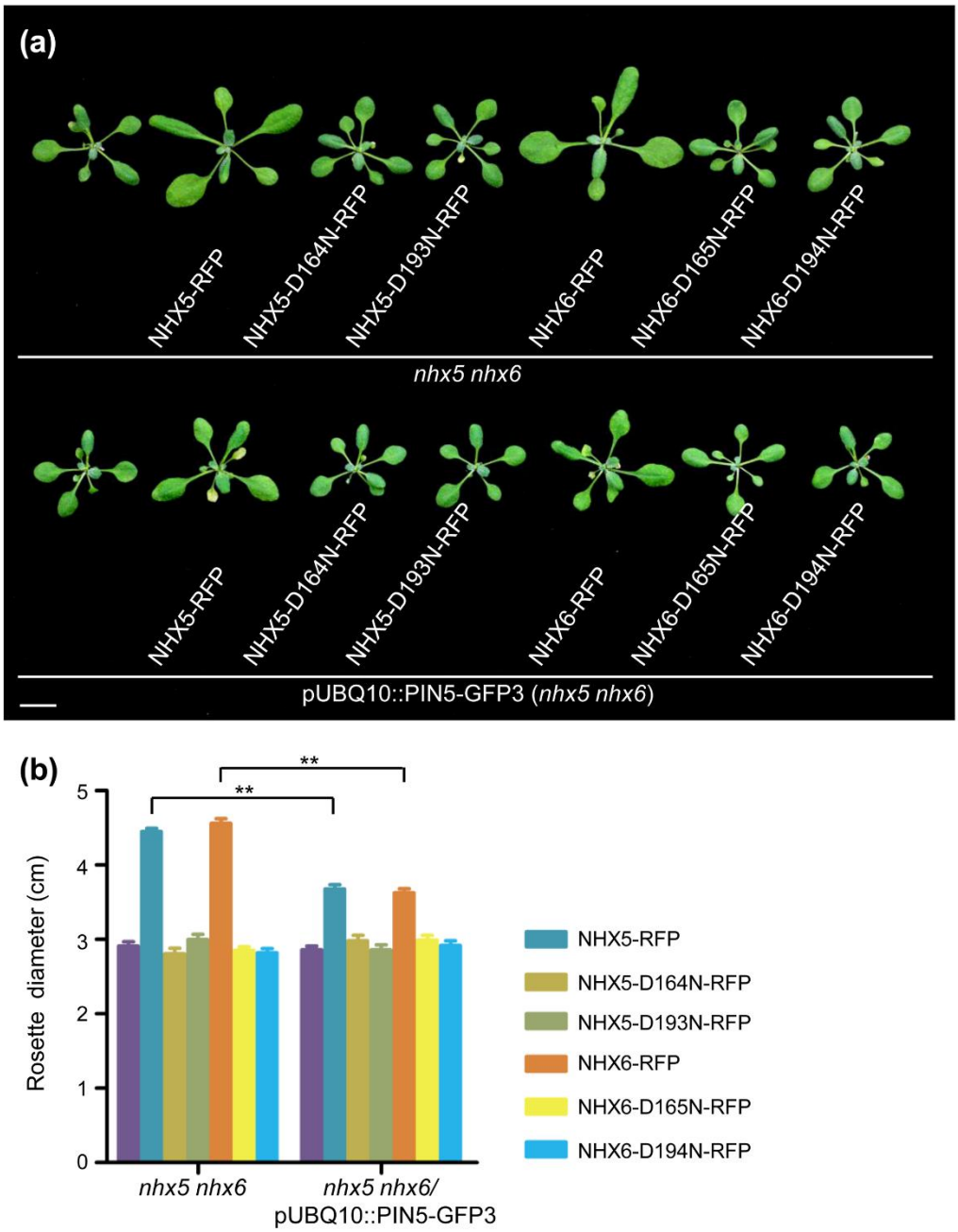

Figure 6. Two conserved acidic resides in AtNHX5 and AtNHX6 are essential for PIN5 function.

(a,b) Phenotype of the transgenic plants. The mutated genes were introduced into the pUBQ10::PIN5-GFP3 line, respectively. Pictures were taken after growing for 2 weeks. (a) Growth of plants. Scale bar, 1 cm. (b) Diameter of the rosettes (mean ± SEM; $n \geqslant 30$). Statistics by *t* test are shown; $^{**}P < 0.01$.

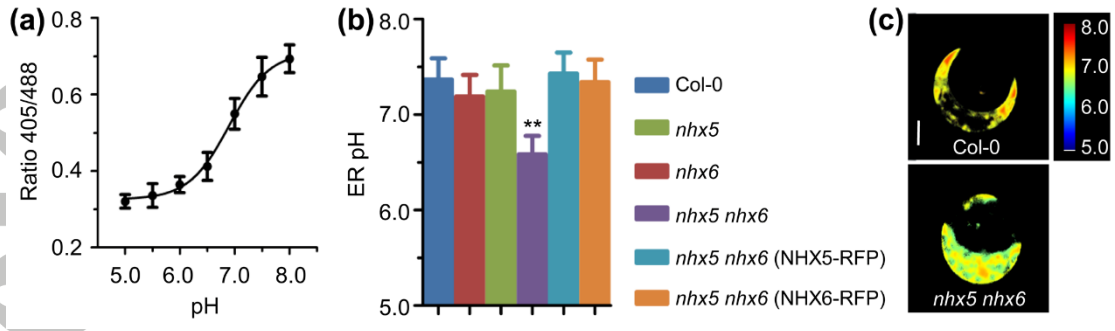

Figure 7. AtNHX5 and AtNHX6 regulate the pH of ER.

(a) In vivo calibration curve of pH in the ER. pH was measured using *Arabidopsis* protoplasts transiently expressing the ER-specific PRpHluorin-HDEL. The images were taken by Leica TCS SP5 confocal microscope. The calibration curve was achieved by equilibrating intracellular pH with 25 μM nigericin, 60 mM KCl, and 10 mM MES/HEPES Bis-Tris-propane, pH 5.0 to 8.0. The data were analyzed by the GraphPad Prism 5 soft. (b) pH of the ER (mean ± SEM; $n \geqslant 20$). Statistics by *t* test are shown; $^{**}P < 0.01$. (c) Representative pseudocolored images of PRpHluorin-HDEL. Scale bar, 20 μm.